

# Dynamical simulation of the fission process and anisotropy of the fission fragment angular distributions of excited nuclei produced in fusion reactions

H. Eslamizadeh\*

*Department of Physics, Persian Gulf University 7516913817 Bushehr, Iran*

(Received 16 July 2016; published 17 October 2016)

**Abstract.** A stochastic approach based on four-dimensional Langevin equations was applied to calculate the anisotropy of fission fragment angular distributions, average pre-scission neutron multiplicity, and the fission probability in a wide range of fissile parameters for the compound nuclei  $^{197}\text{Tl}$ ,  $^{225}\text{Pa}$ ,  $^{248}\text{Cf}$ , and  $^{264}\text{Rf}$  produced in fusion reactions. Three collective shape coordinates plus the projection of total spin of the compound nucleus to the symmetry axis  $K$  were considered in the four-dimensional dynamical model. In the dynamical calculations, nuclear dissipation was generated through the chaos-weighted wall and window friction formula. Furthermore, in the dynamical calculations the dissipation coefficient of  $K$ ,  $\gamma_K$  was considered as a free parameter, and its magnitude inferred by fitting measured data on the anisotropy of fission fragment angular distributions for the compound nuclei  $^{197}\text{Tl}$ ,  $^{225}\text{Pa}$ ,  $^{248}\text{Cf}$ , and  $^{264}\text{Rf}$ . Comparison of the calculated results for the anisotropy of fission fragment angular distributions with the experimental data showed that the results of the calculations are in good agreement with the experimental data by using values of the dissipation coefficient of  $K$  equal to (0.185–0.205), (0.175–0.192), (0.077–0.090), and (0.075–0.085) (MeV zs) $^{-1/2}$  for the compound nuclei  $^{197}\text{Tl}$ ,  $^{225}\text{Pa}$ ,  $^{248}\text{Cf}$ , and  $^{264}\text{Rf}$ , respectively. It was also shown that the influence of the dissipation coefficient of  $K$  on the results of the calculations of the pre-scission neutron multiplicity and fission probability is small.

DOI: [10.1103/PhysRevC.94.044610](https://doi.org/10.1103/PhysRevC.94.044610)

## I. INTRODUCTION

The fission of highly excited compound nuclei formed in heavy-ion-induced fusion reactions is a topic of great interest in nuclear physics. Different features of heavy-ion fusion-fission reactions can be studied by using dynamical or statistical models (see, for example, Refs. [1–18]). During the past three decades the dynamical models based on the set of multidimensional Langevin equations or multidimensional Fokker-Planck equation have been extensively and rather successfully used to solve many problems of collective nuclear dynamics in heavy-ion fusion-fission reactions. The Fokker-Planck equation is a partial differential equation, and it can be solved on the basis of numerical methods only by considering various assumptions, but Langevin equations can be solved without considering additional assumptions.

Many authors for the description of different features of fusion-fission reactions in statistical or dynamical models assumed that compound nuclei have zero spin about the symmetry axis ( $K = 0$ ) where this assumption is not consistent with the statistical model and with dynamical treatment of the orientation degree of freedom, the  $K$  coordinate, as first pointed out by Lestone in Ref. [19]. The authors in Ref. [20] also stressed that a large volume of heavy-ion-induced fission data needs to be reanalyzed using a dynamical treatment of the orientation degree of freedom  $K$ .

In the present paper, I use the four-dimensional dynamical model based on Langevin equations to simulate the dynamics of nuclear fission of the compound nuclei  $^{197}\text{Tl}$ ,  $^{225}\text{Pa}$ ,  $^{248}\text{Cf}$ , and  $^{264}\text{Rf}$  produced in the reactions  $^{16}\text{O} + ^{181}\text{Ta}$ ,  $^{16}\text{O} + ^{209}\text{Bi}$ ,  $^{16}\text{O} + ^{232}\text{Th}$ , and  $^{16}\text{O} + ^{248}\text{Cm}$ ,

respectively. In my simulations, I consider the effect of the evolution of the  $K$  coordinate on the results of dynamical calculations. Furthermore, in my dynamical calculations, I consider the dissipation coefficient of  $K$ ,  $\gamma_K$  as a free parameter, and its magnitude is inferred by fitting measured data on the anisotropy of fission fragment angular distributions for the compound nuclei  $^{197}\text{Tl}$ ,  $^{225}\text{Pa}$ ,  $^{248}\text{Cf}$ , and  $^{264}\text{Rf}$ . It should be stressed that the observable determined by the dynamical evolution of the  $K$  coordinate is the fission fragment angular distribution. Therefore, in the present paper I study the fission fragment angular distributions for the compound nuclei  $^{197}\text{Tl}$ ,  $^{225}\text{Pa}$ ,  $^{248}\text{Cf}$ , and  $^{264}\text{Rf}$ .

The present paper has been arranged as follows. In Sec. II, I describe the models and basic equations. The results of the calculations are presented in Sec. III. Finally, the concluding remarks are given in Sec. IV.

## II. DETAILS OF THE MODELS AND BASIC EQUATIONS

In the four-dimensional (4D) dynamical calculations, I use the three-dimensional Langevin dynamical model that was developed in Refs. [21–23] by adding the orientation degree of freedom ( $K$  coordinate) to three collective coordinates  $\{c, h, \alpha\}$  [24].  $K$  is the projection of the total spin  $I$  to the symmetry (elongation) axis of the nucleus. The coordinate  $c$  describes the elongation of a nucleus; the coordinate  $h$  determines the change in the neck thickness at a given elongation, whereas the coordinate  $\alpha$  specifies the mass ratio for would be fragments. In cylindrical coordinates the surface of the nucleus is given by

$$\rho_s^2(z) = \begin{cases} (c^2 - z^2)(A_s + Bz^2/c^2 + \alpha z/c), & B \geq 0, \\ (c^2 - z^2)(A_s + \alpha z/c) \exp(Bcz^2), & B < 0, \end{cases} \quad (1)$$

Corresponding author: [m\\_eslamizadeh@yahoo.com](mailto:m_eslamizadeh@yahoo.com)

where  $\rho_s$  is the radial coordinate of the nuclear surface and  $z$  is the coordinate along the symmetry axis. The quantities  $A_s$  and  $B$  can be determined as follows:

$$B = 2h + \frac{c-1}{2}, \quad (2)$$

$$A_s = \begin{cases} c^{-3} - \frac{B}{5}, & B \geq 0, \\ -\frac{4}{3} \frac{B}{\exp(Bc^3) + \left(1 + \frac{1}{2Bc^3}\right) \sqrt{-\pi Bc^3 \operatorname{erf}(\sqrt{-Bc^3})}}, & B < 0, \end{cases} \quad (3)$$

where  $\operatorname{erf}(x)$  is the error function.

The evolution of the above-mentioned shape coordinates can be calculated by the coupled Langevin equations of motion,

$$\begin{aligned} \dot{q}_i &= \mu_{ij} p_j, \\ \dot{p}_i &= -\frac{1}{2} p_j p_k \frac{\partial \mu_{jk}}{\partial q_i} - \frac{\partial F}{\partial q_i} - \gamma_{ij} \mu_{jk} p_k + \theta_{ij} \xi_j, \end{aligned} \quad (4)$$

where  $\mathbf{q} = (c, h, \alpha)$  are the collective coordinates,  $\mathbf{p} = (p_c, p_h, p_\alpha)$  are the momenta conjugate to them,  $m_{ij} (\|\mu_{ij}\| = \|\mathbf{m}_{ij}\|^{-1})$  is the tensor of inertia,  $F(\mathbf{q}, K) = V(\mathbf{q}, K) - a(\mathbf{q})T^2$  is the Helmholtz free energy,  $V(\mathbf{q}, K)$  is the potential energy,  $\gamma_{ij}$  is the friction tensor,  $\theta_{ij} \xi_j$  is a random force,  $\theta_{ij}$  is its amplitude, and  $\xi_j$  is a random variable that possesses the following statistical properties  $\langle \xi_i \rangle = 0$  and  $\langle \xi_i(t_1) \xi_j(t_2) \rangle = 2\delta_{ij} \delta(t_1 - t_2)$ . The heat bath temperature  $T$  can be determined within the Fermi-gas model as  $T = \sqrt{E_{\text{int}}/a(\mathbf{q})}$ , where  $E_{\text{int}}$  is the intrinsic excitation energy of the nucleus and  $a(\mathbf{q})$  is the level-density parameter. The deformation dependence of the level-density parameter can be determined as  $a(\mathbf{q}) = a_v A + a_s A^{2/3} B_s(\mathbf{q})$  where  $A$  is the mass number of the fissile nucleus and  $B_s$  is the dimensionless functional of the surface energy in the liquid-drop model. In the present paper, I employ the coefficients  $a_v = 0.073$  and  $a_s = 0.095 \text{ MeV}^{-1}$ , which were proposed by Ignatyuk and his coauthors in Ref. [25]. In the present calculations, I use the variables  $\mathbf{q} = (q_1, q_2, q_3)$  as collective coordinates which are connected with the shape parameters  $c, h$ , and  $\alpha$  as follows:

$$\begin{aligned} q_1 &= c, \\ q_2 &= \left(h + \frac{3}{2}\right) / \left(\frac{5}{2c^3} + \frac{1-c}{4} + \frac{3}{2}\right), \\ q_3 &= \alpha / (A_s + B), \quad \text{if } B \geq 0, \\ q_3 &= \alpha / A_s, \quad \text{if } B < 0. \end{aligned} \quad (5)$$

The advantage of using the collective coordinates  $\mathbf{q} = (q_1, q_2, q_3)$  instead of the  $(c, h, \alpha)$  parameters was discussed in Ref. [26].

In my dynamical calculations, I start modeling fission dynamics from the ground state with the excitation energy  $E^*$  of the compound nucleus. The initial conditions for the compound nucleus can be generated by the Neumann method. The initial spin for each Langevin trajectory can be sampled from the spin distribution as in Ref. [27],

$$\sigma(I) = \frac{2\pi}{k^2} \frac{2I+1}{1 + \exp\left(\frac{I-I_c}{\delta I}\right)}, \quad (6)$$

where  $k, I_c$ , and  $\delta I$  are the wave number, the critical spin for fusion, and the diffuseness, respectively.  $I_c$  and  $\delta I$  values

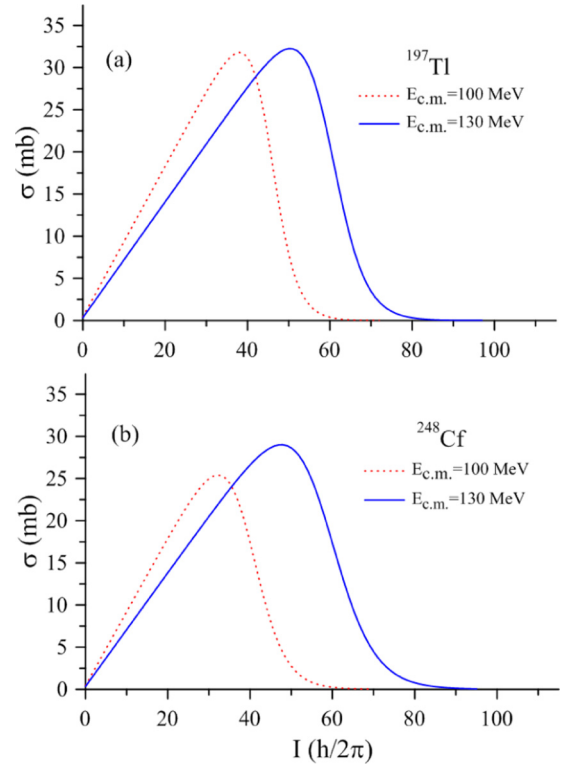


FIG. 1. The cross sections for the reactions  $^{16}\text{O} + ^{181}\text{Ta} \rightarrow ^{197}\text{Tl}$  and  $^{16}\text{O} + ^{232}\text{Th} \rightarrow ^{248}\text{Cf}$  as a function of spin and at projectile energies of 100 and 130 MeV.

can be defined according to the scaled prescription [27]. Figures 1(a) and 1(b) show the cross sections for  $^{197}\text{Tl}$  and  $^{248}\text{Cf}$  as a function of spin and, for example, at projectile energies of 100 and 130 MeV in the center-of-mass system. It is clear from Figs. 1(a) and 1(b) that as the energy of the projectile increases, the value of the spin of the compound nucleus formed increases.

The initial  $K$  value can also be generated using the Monte Carlo method from uniform distribution in the interval  $(-I, I)$ . During a random walk along the Langevin trajectory in the space of the collective coordinates, the conservation of energy is satisfied by  $E^* = E_{\text{int}}(t) + E_{\text{coll}}(\mathbf{q}, \mathbf{p}) + V(\mathbf{q}, K) + E_{\text{evap}}(t)$ , where  $E^*$  is the total excitation energy of the nucleus,  $E_{\text{int}}$  is the intrinsic energy,  $E_{\text{coll}}$  is the kinetic energy of the collective motion of the nucleus, which can be determined by the formula  $E_{\text{coll}} = 0.5\mu_{ij}(\mathbf{q})p_i p_j$ ,  $V(\mathbf{q}, K)$  is the potential energy of the compound nucleus, and  $E_{\text{evap}}(t)$  is the energy carried away by evaporated particles by time  $t$ . The potential energy is calculated on the basis of the liquid-drop model with a finite range of nuclear forces [28] using the parameters from Ref. [29]. Figures 2(a) and 2(b) show the Helmholtz free energy calculated for the compound nuclei  $^{197}\text{Tl}$  and  $^{248}\text{Cf}$  as a function of the collective coordinate  $q_1$  and  $K$  values at  $T = 2 \text{ MeV}$ .

It can be seen from Figs. 2(a) and 2(b) that the inclusion of the  $K$  coordinate not only changes the fission barrier height, but also affects the saddle-point configuration. Moreover, the inclusion of the  $K$  coordinate in the calculation of the potential

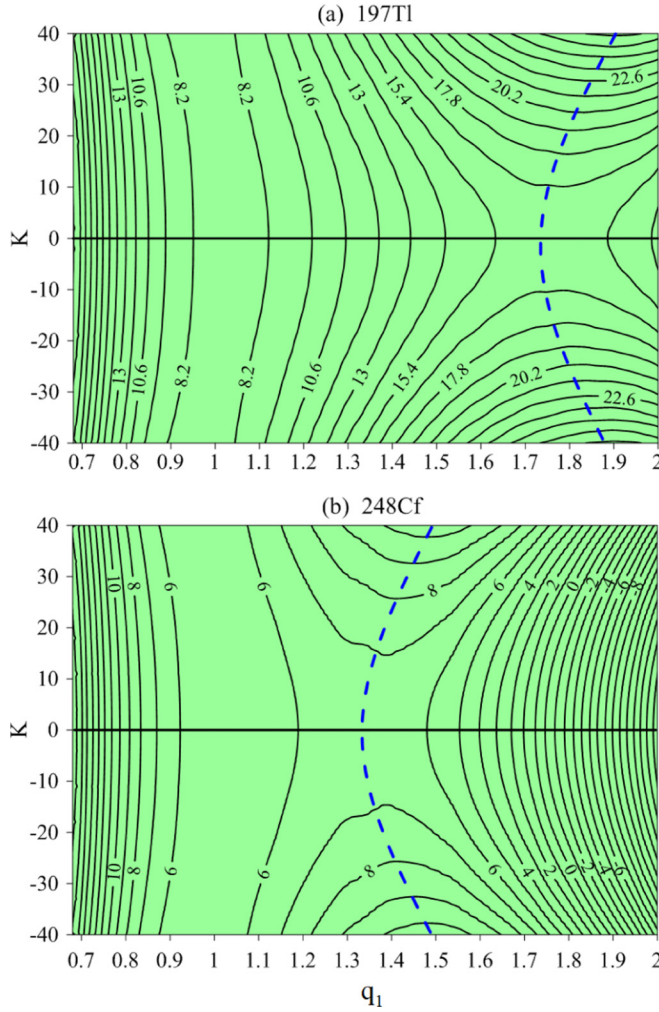


FIG. 2. The Helmholtz free energies for the compound nuclei  $^{197}\text{Tl}$  and  $^{248}\text{Cf}$  as a function of the collective coordinates  $q_1$  and  $K$  at  $T = 2\text{ MeV}$  and  $I = 40\hbar$ . The dashed line curves show the dependence of saddle-point deformations on  $K$ . The numbers on the contour lines represent the potential-energy surface values in MeV.

energy shifts the saddle point toward the scission point. It is also clear from Fig. 2(a) that for the lighter nucleus  $^{197}\text{Tl}$  the saddle point is closer to the scission point. It should be mentioned that in the present paper the potential energy is calculated on a macroscopic basis via the liquid-drop model. To have a complete picture of the fission phenomenon, it is necessary to add the microscopic corrections (shell and pairing) to the potential energy. Although, it is possible to neglect shell effects and the nucleon-pairing effect at high excitation energies. This is because the possible correction magnitude of the potential energy is about a couple of MeV for shell and pairing effects. The influence of shell corrections on fission was also treated within microscopic models, such as the deformed two-center potential ones in Refs. [30,31].

In the calculations, nuclear dissipation is generated through the chaos-weighted wall and window friction formula. For small elongation before neck formation, I use the chaos-weighted wall formula, and after neck formation, I use the

chaos-weighted wall and window friction formula [32–34],

$$\gamma_{ij} = \begin{cases} \mu(\mathbf{q})\gamma_{ij}^{\text{wall}} & \text{for nuclear shapes featuring no neck,} \\ \mu(\mathbf{q})\gamma_{ij}^{\text{wall}} + \gamma_{ij}^{\text{win}} & \text{for nuclear shapes featuring a neck,} \end{cases} \quad (7)$$

where

$$\gamma_{ij}^{\text{win}} = \frac{1}{2}\rho_m \bar{v} \left\{ \left( \frac{\partial R}{\partial q_i} \frac{\partial R}{\partial q_j} \right) \Delta\sigma \right\} \quad (8)$$

for nuclear shapes featuring no neck,

$$\gamma_{ij}^{\text{wall}} = \frac{\pi\rho_m}{2} \bar{v} \int_{z_{\min}}^{z_{\max}} \left( \frac{\partial \rho_s^2}{\partial q_i} \right) \left( \frac{\partial \rho_s^2}{\partial q_j} \right) \times \left[ \rho_s^2 + \left( \frac{1}{2} \frac{\partial \rho_s^2}{\partial z} \right)^2 \right]^{-1/2} dz, \quad (9)$$

and for nuclear shapes featuring a neck,

$$\gamma_{ij}^{\text{wall}} = \frac{\pi\rho_m}{2} \bar{v} \left\{ \int_{z_{\min}}^{z_N} \left( \frac{\partial \rho_s^2}{\partial q_i} + \frac{\partial \rho_s^2}{\partial z} \frac{\partial D_1}{\partial q_i} \right) \left( \frac{\partial \rho_s^2}{\partial q_j} + \frac{\partial \rho_s^2}{\partial z} \frac{\partial D_1}{\partial q_j} \right) \times \left[ \rho_s^2 + \left( \frac{1}{2} \frac{\partial \rho_s^2}{\partial z} \right)^2 \right]^{-1/2} dz + \int_{z_N}^{z_{\max}} \left( \frac{\partial \rho_s^2}{\partial q_i} + \frac{\partial \rho_s^2}{\partial z} \frac{\partial D_2}{\partial q_i} \right) \times \left( \frac{\partial \rho_s^2}{\partial q_j} + \frac{\partial \rho_s^2}{\partial z} \frac{\partial D_2}{\partial q_j} \right) \left[ \rho_s^2 + \left( \frac{1}{2} \frac{\partial \rho_s^2}{\partial z} \right)^2 \right]^{-1/2} dz \right\}, \quad (10)$$

where  $\rho_m$  is the mass density of the nucleus,  $\rho_s$  is the radial coordinate of the nuclear surface,  $z_N$  is the position of the neck plane that divides the nucleus into two parts,  $z_{\min}$  and  $z_{\max}$  are the left and right ends of the nuclear shape,  $\bar{v}$  is the average nucleon speed inside the nucleus,  $D_1$  and  $D_2$  are the positions of the mass centers of the two parts of the fissioning system relative to the center of mass of the whole system,  $R$  is the distance between the centers of mass of future fragments, and  $\Delta\sigma$  is an area of the window between two parts of the system.

In Eq. (7), the chaoticity  $\mu$  is a measure of chaos in the single-particle motion and depends on the shape of the nucleus. The magnitude of chaoticity  $\mu$  changes from 0 to 1 as the nucleus evolves from a spherical to a deformed shape.

The inertia tensor is calculated in the Werner-Wheeler approximation for the incompressible and irrotational flows [35]. It was shown in Ref. [36] that this method makes it possible to calculate accurately the components of the tensor of inertia for all shapes of the nucleus undergoing fission with the exception of the zero neck radius configurations. It should be mentioned that the Werner-Wheeler approximation does not include the changes within the energy-level scheme with deformation. In theoretical calculations, this simplification can increase the fission probability. Furthermore, this simplification can slightly decrease the pre-scission neutron multiplicity and anisotropy of fission fragment angular distributions for excited nuclei.

The decay widths for emission  $n, p, \alpha, \gamma$  are calculated at each Langevin time step  $\Delta t$ . The probabilities of decay via different channels can be calculated by using a standard Monte Carlo cascade procedure where the kind of decay is selected with the weights  $\Gamma_v/\Gamma_{\text{tot}}$  with  $v = n, p, \alpha, \gamma$  and  $\Gamma_{\text{tot}} = \sum_v \Gamma_v$ . After the particle type is randomly chosen, the kinetic energy  $\varepsilon_v$  of the emitted particle is also generated via a Monte Carlo procedure. Then the intrinsic excitation energy, mass, and spin of the residual compound nucleus are recalculated, and the dynamics is continued. The loss of angular momentum is taken into account by assuming that each neutron, proton, or  $\gamma$  quanta carries away  $1\hbar$  whereas the  $\alpha$  particle carries away  $2\hbar$ . In the simulation of the evolution of a fissile nucleus a Langevin trajectory either reaches the scission point in which case it is counted as a fission event, or if the excitation energy for a trajectory which is still inside the saddle reaches the value  $E_{\text{int}} + E_{\text{coll}} < \min(B_v, B_f)$ , the event is counted as an evaporation residue ( $B_v$  is the binding energy of the particle  $v = n, p, \alpha$ , and  $B_f$  is the fission barrier height).

The average values of the pre-scission neutron multiplicity can be determined by using the following relation:

$$\langle O \rangle = \frac{\sum_{I=0}^{I_{\text{cr}}} \sum_{\alpha=0}^{\alpha_f} \langle O \rangle_{I\alpha} (2I+1) P_I}{\sum_{I,\alpha} (2I+1) P_I}, \quad (11)$$

where  $\alpha_f$  and  $I_{\text{cr}}$  are the maximum asymmetry parameter and the critical spin for fusion, respectively.  $P_I$  is the probability of a particle crossing the fission barrier, which depends upon spin, and is calculated using  $P_I = N_f/N$ . The quantities  $N_f$  and  $N$  are the number of trajectories which undergo fission for given  $\alpha, I$ , and the total number of trajectories, respectively. In the calculations, it is assumed that the separation of a compound nucleus into two fragments occurs at a neck radius of  $0.3R_0$  on average [24,37,38] ( $R_0$  is the radius of the spherical nucleus).

In the present paper, I use the 4D dynamical model and standard transition state model [39–41] to analyze the fission fragment angular distributions. In analyzing the fission fragment angular distributions, it is usually assumed that fission fragments travel in the direction of the symmetry axis of the nucleus. Consequently, the fission fragment angular distributions can be determined by three quantum numbers:  $I$ ,  $M$ , and  $K$ , where  $I$  is the total spin of a compound nucleus,  $M$  is the projection of the total spin on the axis of the projectile ion beam, and  $K$  is the projection of  $I$  on the symmetry axis of the nucleus. In the case of fusion of spinless ions, one finds  $M = 0$ . Furthermore, in the case of heavy-ion-induced fission reactions, the spin of the compound nucleus is usually much larger than the ground-state spins of the target and projectile and is perpendicular to the beam axis so that  $M = 0$ . Hence, the fission fragment angular distributions can be obtained by the following relation [39,40]:

$$W(\theta, I, K) = (I + 1/2) |D_{M=0, K}^I(\theta)|^2, \quad (12)$$

where  $\theta$  is the angle with respect to the space fixed axis and  $D_{M, K}^I(\theta)$  is the symmetric-top-wave function [39]. In the dynamical calculations, the fission fragment angular distributions can be obtained by averaging the expression

Eq. (12) over the ensemble of Langevin trajectories as follows:

$$W(\theta) = \frac{1}{N_f} \sum_{i=1}^{N_f} (I^i + 1/2) |D_{0, K^i}^{I^i}(\theta)|^2, \quad (13)$$

where upper index  $i$  determines the value of the corresponding quantity at the scission point for the  $i$ th Langevin trajectory and  $N_f$  is the number of trajectories reaching the scission surface.

The fission fragment angular distributions can also be calculated on the basis of the standard transition state model [39–41]. This model assumes that there is a certain transition configuration for a fissile system that one can use to determine the fission fragment angular distributions. There are two assumptions on the position of the transition state, and consequently one can consider two variants of the transition state model. These models are the saddle-point transition model (SPTS) [39–41] and the scission-point transition model (SCTS) [42–44]. Important assumptions of the saddle-point transition model are as follows: (1) the mean time of stay of a nucleus in the saddle-point region is sufficiently larger than a characteristic time of the equilibration of the  $K$  mode, (2) the mean time of the descent of a nucleus from the saddle point to the scission point is short in comparison with the characteristic time of the equilibration of the  $K$  mode, and (3) a Gaussian distribution can be considered for  $K$  in the saddle point. In the standard transition state model at high values of  $I$ ,  $W(\theta, I, K)$  can be approximated as

$$W(\theta, I, K) \approx \frac{I + 1/2}{\pi} [(I + 1/2)^2 \sin^2 \theta - K^2]^{1/2}. \quad (14)$$

The fission fragment angular distributions can be calculated by averaging expression Eq. (14) with the distributions of  $I$  and  $K$  as follows:

$$W(\theta) = \sum_{I=0}^{\infty} \sigma_I \sum_{K=-I}^I P(K) W(\theta, I, K), \quad (15)$$

where  $\sigma_I$  and  $P(K)$  are the distributions of compound nuclei with respect to the total spin and its projection, respectively. In order to calculate the angular distributions of compound nuclei, it is necessary to specify the type of the distribution  $\sigma_I$  and  $P(K)$  of the compound nuclei over  $I$  and  $K$ , respectively. In the saddle-point transition state model, an equilibrium distribution of  $K$  values is assumed at the saddle point. This distribution can be determined by the Boltzmann factor  $\exp(-E_{\text{rot}}/T)$  [41]. Therefore, the equilibrium distribution with respect to  $K$  has the form

$$P_{ep}(K) = \frac{\exp[-K^2/(2K_0^2)]}{\sum_{K=-I}^I \exp[-K^2/(2K_0^2)]}, \quad (16)$$

where the variance of the equilibrium  $K$  distribution  $K_0$  is given by the following relation:

$$K_0^2 = \frac{T}{\hbar^2} J_{\text{eff}}, \quad J_{\text{eff}} = \frac{J_{\parallel} J_{\perp}}{J_{\perp} - J_{\parallel}}, \quad (17)$$

where  $T$ ,  $J_{\parallel}$ , and  $J_{\perp}$  are the nuclear temperature and the parallel and perpendicular moments of inertia taken at the transition state. One can obtain an expression for the fission fragment

angular distributions for a fixed  $I$  by averaging Eq. (14) as follows:

$$W(\theta, I) = (I + 1/2) \frac{\sum_{K=-I}^I |D'_{0,K}(\theta)| \exp(-K^2/2K_0^2)}{\sum_{K=-I}^I \exp(-K^2/2K_0^2)} \approx \sqrt{\frac{2p}{\pi}} \frac{\exp(-p \sin^2 \theta) J_0(-p \sin^2 \theta)}{\text{erf}(\sqrt{2p})}, \quad (18)$$

where  $J_0$  is a Bessel function of zero order and  $p = (I + 1/2)^2/(4K_0^2)$ . The anisotropy of fission fragment angular distributions can be defined as

$$A = \frac{\langle W(0^\circ) \rangle}{\langle W(90^\circ) \rangle}. \quad (19)$$

In the case of  $p \gg 1$  the anisotropy of fission fragment angular distributions can be obtained by the approximate relation,

$$A \approx 1 + \frac{\langle I^2 \rangle}{4K_0^2}. \quad (20)$$

An expression similar to Eq. (18) can also be used in the scission-point transition model, but factors determined by Eq. (17) should be calculated at the scission point. In the scission-point model, it is assumed that the characteristic time of the equilibration of the  $K$  mode is much shorter than the descent time from the saddle point to the scission point. In this case the equilibration of the  $K$  degree of freedom is supposed to be at the scission point. It should be noted that, for the calculation of the anisotropy of fission fragment angular distributions,  $W(\theta)$  was obtained either from the 4D dynamical model using Eq. (13) or from the transition state model using Eq. (15).

In the present dynamical calculations, I do not use any approximation about the relaxation time for the  $K$  coordinate to analyze the fission fragment angular distributions according to Eq. (13). Instead, I directly treat the relaxation time for the  $K$  coordinate using the following equation [45]:

$$dK = -\frac{\gamma_K^2 I^2}{2} \frac{\partial V}{\partial K} dt + \gamma_K I \xi(t) \sqrt{T} dt, \quad (21)$$

and take into account the influence of the actual evolution of the  $K$  value on the dynamics of the shape parameters ( $q_1, q_2, q_3$ ). In Eq. (21) the dissipation coefficient of  $K, \gamma_K$  is a parameter controlling the coupling between the orientation degree of freedom  $K$  and the heat bath, and  $\xi(t)$  has the same meaning as in Eq. (4). The authors in Refs. [20,45], based on the works of Døssing and Randrup [46] and Randrup [47], have shown that in the case of a dinucleus,  $\gamma_K$  can be obtained as

$$\gamma_K = \frac{1}{RR_N \sqrt{2\pi^3 n_0}} \sqrt{\frac{J_R |J_{\text{eff}}| J_{\parallel}}{J_{\perp}^3}}, \quad (22)$$

where  $n_0 = 0.0263 \text{ MeV zs fm}^{-4}$  is the bulk flux in the standard nuclear matter [46],  $R$  is the distance between the centers of mass of the nascent fragments, and  $R_N$  is the neck radius.  $J_R = M_0 R^2/4$  for a reflection symmetric shape, and  $J_{\text{eff}}$  is the effective moment of inertia. The inverse of the effective moment of inertia is  $J_{\text{eff}}^{-1} = J_{\parallel}^{-1} - J_{\perp}^{-1}$ . The rigid body moments of inertia about and perpendicular to the symmetry

axis can be determined as in Ref. [48]. It should be mentioned that the Langevin equation for the  $K$  coordinate Eq. (21) and the Langevin equations Eq. (4) are connected through the potential energy. The rotational part of the potential energy is calculated by

$$E_{\text{rot}}(\mathbf{q}, I, K) = \frac{\hbar^2 I(I+1)}{2J_{\perp}(\mathbf{q})} + \frac{\hbar^2 K^2}{2J_{\text{eff}}(\mathbf{q})}. \quad (23)$$

By averaging Eq. (21), it can be shown that

$$\frac{d\langle K \rangle}{dt} = -\frac{\gamma_K^2 I^2}{2} \left\langle \frac{\partial V}{\partial K} \right\rangle. \quad (24)$$

From the expression for the rotational energy Eq. (23), it follows that:

$$\frac{d\langle K \rangle}{dt} = -\frac{\gamma_K^2 I^2 \hbar^2}{2J_{\text{eff}}} \langle K \rangle. \quad (25)$$

By assuming a constant  $\gamma_K$ , the solution of this equation is

$$\langle K(t) \rangle_{K_0} = K_0 \exp \left[ -\frac{\gamma_K^2 I^2 \hbar^2}{2J_{\text{eff}}} (t - t_0) \right], \quad (26)$$

which gives the following expression for the relaxation time as:

$$\tau_K = \frac{2J_{\text{eff}}}{\gamma_K^2 I^2 \hbar^2}. \quad (27)$$

It is clear from Eq. (27) that the relaxation time of the  $K$  coordinate decreases with increasing  $\gamma_K$ .

### III. RESULTS AND DISCUSSIONS

In the present paper, a stochastic approach based on 4D Langevin equations has been used to calculate the anisotropy of fission fragment angular distributions, average pre-scission neutron multiplicity, and the fission probability for the compound nuclei  $^{197}\text{Tl}$ ,  $^{225}\text{Pa}$ ,  $^{248}\text{Cf}$ , and  $^{264}\text{Rf}$  produced in the reactions  $^{16}\text{O} + ^{181}\text{Ta}$ ,  $^{16}\text{O} + ^{209}\text{Bi}$ ,  $^{16}\text{O} + ^{232}\text{Th}$ , and  $^{16}\text{O} + ^{248}\text{Cm}$ , respectively. In the 4D dynamical calculations, the dissipation coefficient of  $K, \gamma_K$  has been considered as a free parameter, and its magnitude inferred by fitting measured data on the anisotropy of fission fragment angular distributions for the compound nuclei  $^{197}\text{Tl}$ ,  $^{225}\text{Pa}$ ,  $^{248}\text{Cf}$ , and  $^{264}\text{Rf}$ . Figures 3(a)–3(d) show the results of anisotropy of the fission fragment angular distributions calculated with the 4D dynamical model and by using values of the dissipation coefficient of  $K$  equal to (0.185–0.205), (0.175–0.192), (0.077–0.090), and (0.075–0.085) (MeV zs) $^{-1/2}$  for the compound nuclei  $^{197}\text{Tl}$ ,  $^{225}\text{Pa}$ ,  $^{248}\text{Cf}$ , and  $^{264}\text{Rf}$ , respectively. Figures 3(a)–3(d) also show the results of the transition state model for the anisotropy of fission fragment angular distributions calculated at the saddle and scission points.

It can be seen from Figs. 3(a)–3(d) that the increase in  $\gamma_K$  increases the anisotropy of fission fragment angular distributions. It can be explained by considering Eq. (27) for the relaxation time of the  $K$  collective coordinate. The larger  $\gamma_K$  value causes a faster relaxation time of the  $K$  coordinate and a narrower  $K$  distribution, which corresponds to the large  $A$  values as can be seen from Eq. (20). It can also be seen from Figs. 3(a)–3(d) that neither the saddle-point

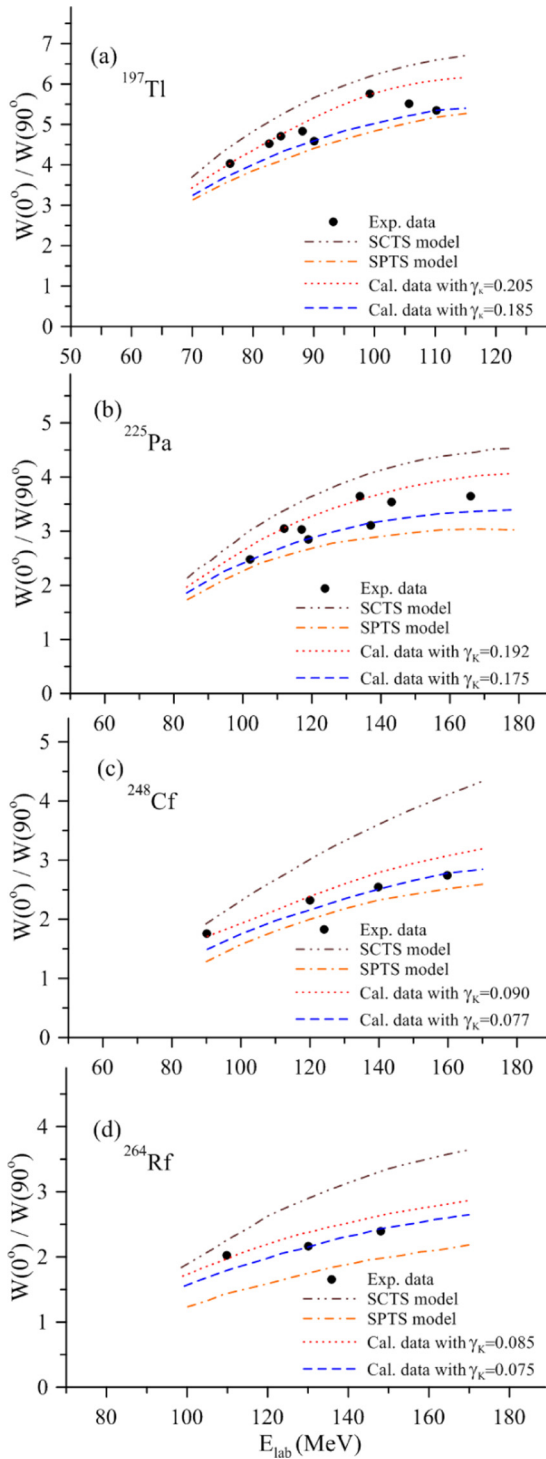


FIG. 3. The anisotropy of fission fragment angular distributions for the compound nuclei  $^{197}\text{Tl}$ ,  $^{225}\text{Pa}$ ,  $^{248}\text{Cf}$ , and  $^{264}\text{Rf}$  as a function of projectile energy in the laboratory system. The filled circles are the experimental data [49–53]. The dashed and dotted curves correspond to fitted values calculated with the 4D dynamical model and by using different values of  $\gamma_K$ . The dashed-dotted and dashed-double-dotted curves correspond to fitted values calculated by the SPTS and SCTS models, respectively.

transition state model nor the scission-point state model is able to provide a satisfactory description on the anisotropy

of fission fragment angular distributions for the compound nuclei  $^{197}\text{Tl}$ ,  $^{225}\text{Pa}$ ,  $^{248}\text{Cf}$ , and  $^{264}\text{Rf}$ . Therefore, the existing

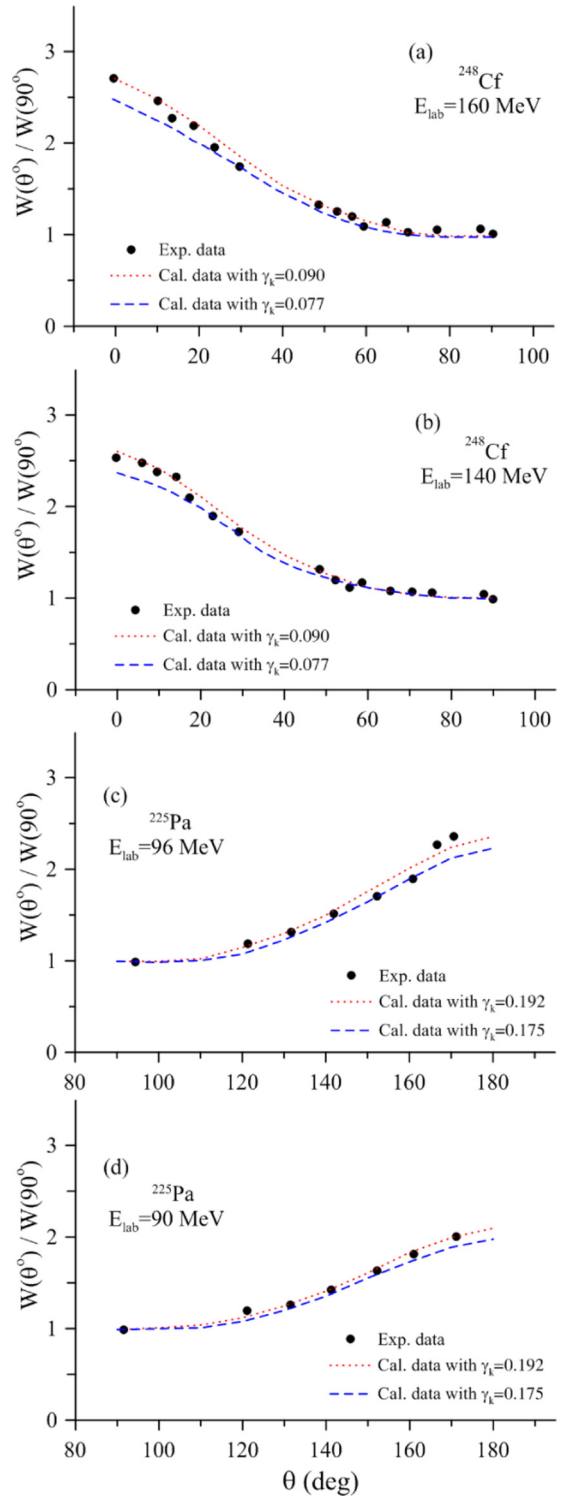


FIG. 4. The anisotropy of fission fragment angular distributions for the compound nuclei  $^{225}\text{Pa}$  and  $^{248}\text{Cf}$  as a function of the scattering angle and at different values of projectile energy in the laboratory system. The curves correspond to fitted values calculated with the 4D dynamical model and by using different values of  $\gamma_K$ . The experimental data (filled circles) are taken from Refs. [53,54].

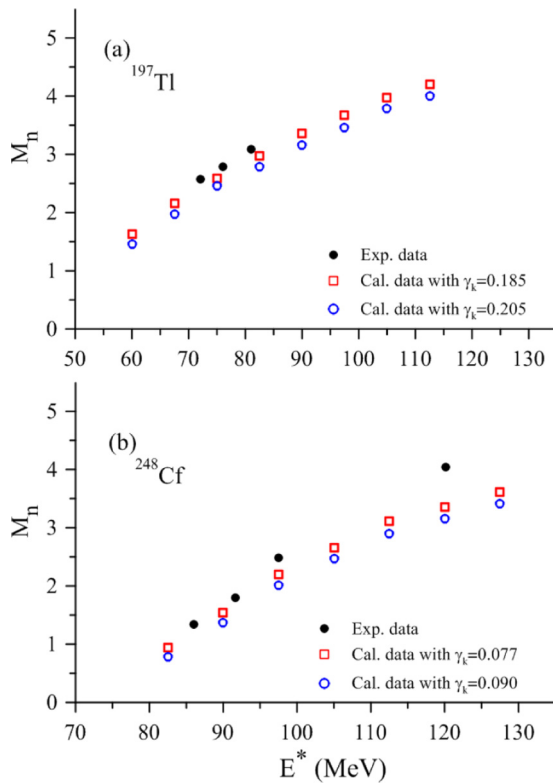


FIG. 5. The average precession neutron multiplicity for the compound nuclei  $^{197}\text{Tl}$  and  $^{248}\text{Cf}$  as a function of excitation energy and different values of  $\gamma_K$ . The experimental data (filled circles) are taken from Refs. [55,56].

uncertainty in the position of the transition state indicates that it is necessary to take into account dynamical features of the formation of angular distributions and it is necessary to treat  $K$  as an independent collective coordinate. In the present paper, I have also calculated the anisotropy of fission fragment angular distributions as a function of scattering angle and at different values of projectile energy for the compound nuclei  $^{225}\text{Pa}$  and  $^{248}\text{Cf}$ . Figures 4(a)–4(d) show the results of anisotropy of the fission fragment angular distributions as a function of the scattering angle calculated with the 4D dynamical model and by using values of the dissipation coefficient of  $K$  equal to (0.175–0.192) and (0.077–0.090)  $(\text{MeV zs})^{-1/2}$  for the compound nuclei  $^{225}\text{Pa}$  and  $^{248}\text{Cf}$ , respectively. It is clear from Figs. 4(a)–4(d) that the results of the 4D dynamical model are compatible with the experimental data.

In the present paper, I have also studied the effect of the dissipation coefficient of  $K$  on the average precession neutron multiplicity and fission probability for the compound nuclei  $^{197}\text{Tl}$ ,  $^{225}\text{Pa}$ ,  $^{248}\text{Cf}$ , and  $^{264}\text{Rf}$ . Figures 5(a) and 5(b) show the results of average precession neutron multiplicity for the compound nuclei  $^{197}\text{Tl}$  and  $^{248}\text{Cf}$ , and Fig. 6 shows the results of fission probability calculated with the 4D dynamical model and by using values of the dissipation coefficient of  $K$  equal to (0.185–0.205), (0.175–0.192), (0.077–0.090), and (0.075–0.085)  $(\text{MeV zs})^{-1/2}$  for the compound nuclei  $^{197}\text{Tl}$ ,  $^{225}\text{Pa}$ ,  $^{248}\text{Cf}$ , and  $^{264}\text{Rf}$ , respectively.

It is clear from Fig. 5(b) that the results of neutron multiplicity for  $^{248}\text{Cf}$  lay somewhat below the experimental

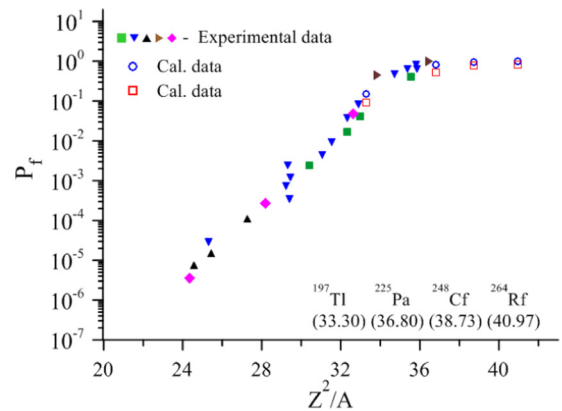


FIG. 6. Results of the calculations for fission probabilities as a function of the parameter  $Z^2/A$ . The open squares and open circles are the calculated results calculated with the 4D dynamical model and by using different values of  $\gamma_K$  which were extracted in the present paper for the compound nuclei  $^{197}\text{Tl}$ ,  $^{225}\text{Pa}$ ,  $^{248}\text{Cf}$ , and  $^{264}\text{Rf}$ . The closed symbols are the experimental data [57–59].

data at high excitation energies. It can be concluded that for heavy nuclei the strength of the nuclear dissipation needs to be increased to reproduce the measured precession neutron multiplicity. It can also be seen from Figs. 5(a), 5(b), and 6 that the differences between the calculated data obtained with different values of  $\gamma_K$  are small.

Finally, it would be useful to compare the extracted values of the dissipation coefficient of  $K$  for the compound nuclei  $^{197}\text{Tl}$ ,  $^{225}\text{Pa}$ ,  $^{248}\text{Cf}$ , and  $^{264}\text{Rf}$  which are studied in the present paper. Figure 7 shows the extracted values of the dissipation coefficients of  $K$  as a function of compound nucleus mass number.

#### IV. CONCLUSIONS

The anisotropies of the fission fragment angular distributions have been calculated in the framework of the 4D dynamical model for the compound nuclei  $^{197}\text{Tl}$ ,  $^{225}\text{Pa}$ ,  $^{248}\text{Cf}$ ,

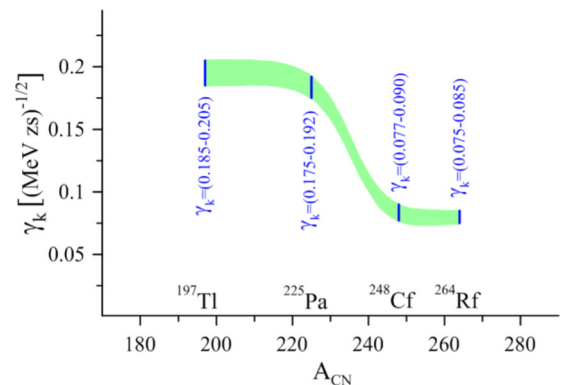


FIG. 7. The extracted values of the dissipation coefficient of  $K$  (solid lines) for the compound nuclei  $^{197}\text{Tl}$ ,  $^{225}\text{Pa}$ ,  $^{248}\text{Cf}$ , and  $^{264}\text{Rf}$ . The shaded area represents the variation of the best-fit values of the dissipation coefficient of  $K$  with the compound nucleus mass number.

and  $^{264}\text{Rf}$  produced in fusion reactions, and the results of the calculations have been compared with the experimental data. The chaos-weighted wall and the window friction formulas have been used in Langevin equations. Furthermore, in the calculations the dissipation coefficient of  $K$ ,  $\gamma_k$  is considered as a free parameter, and its magnitude inferred by fitting measured data on the anisotropy of fission fragment angular distributions for the compound nuclei  $^{197}\text{Tl}$ ,  $^{225}\text{Pa}$ ,  $^{248}\text{Cf}$ , and  $^{264}\text{Rf}$ . Comparison of the theoretical results for the anisotropy of fission fragment angular distributions with the experimental data showed that the results of the calculations are in good agreement with the experimental data by using values of the dissipation coefficient of  $K$  equal to (0.185–0.205), (0.175–0.192), (0.077–0.090), and (0.075–0.085)  $(\text{MeV zs})^{-1/2}$  for the compound nuclei  $^{197}\text{Tl}$ ,  $^{225}\text{Pa}$ ,  $^{248}\text{Cf}$ , and  $^{264}\text{Rf}$ , respectively.

The effect of the dissipation coefficient of  $K$  has also been investigated on the estimation of the average precession neutron multiplicity and fission probability for the above-mentioned nuclei. It was shown that the difference between the results of the calculations calculated with different values of the dissipation coefficient of  $K$  is small. It was also shown that at high excitation energies the results of neutron multiplicities for the heavy nucleus  $^{248}\text{Cf}$  are slightly lower than the experimental data. According to the obtained results, it can be concluded that, for heavy nuclei, the strength of the nuclear dissipation needs to be increased.

#### ACKNOWLEDGMENT

Support from the Research Committee of the Persian Gulf University is greatly acknowledged.

- 
- [1] P. N. Nadtochy, E. G. Ryabov, A. E. Gegechkori, Y. A. Anischenko, and G. D. Adeev, *Phys. Rev. C* **89**, 014616 (2014).
- [2] P. N. Nadtochy, E. G. Ryabov, A. E. Gegechkori, Y. A. Anischenko, and G. D. Adeev, *Phys. Rev. C* **85**, 064619 (2012).
- [3] J. P. Lestone, J. R. Leigh, J. O. Newton, D. J. Hinde, J. X. Wei, J. X. Chen, S. Elfström, and M. Zielinska-Pfabé, *Nucl. Phys. A* **559**, 277 (1993).
- [4] H. Eslamizadeh, *J. Phys. G: Nucl. Part. Phys.* **42**, 095103 (2015).
- [5] W. Ye and J. Tian, *Phys. Rev. C* **93**, 044603 (2016).
- [6] W. Ye and J. Tian, *Phys. Rev. C* **91**, 064603 (2015).
- [7] H. Eslamizadeh, *Eur. Phys. J. A* **50**, 186 (2014).
- [8] J. Tian, N. Wang, and W. Ye, *Chin. Phys. C* **39**, 034102 (2015).
- [9] N. Vonta, G. A. Souliotis, M. Veselsky, and A. Bonasera, *Phys. Rev. C* **92**, 024616 (2015).
- [10] M. V. Borunov, P. N. Nadtochy, and G. D. Adeev, *Nucl. Phys. A* **799**, 56 (2008).
- [11] D. V. Vanin, G. I. Kosenko, and G. D. Adeev, *Phys. Rev. C* **59**, 2114 (1999).
- [12] A. Gavron, *Phys. Rev. C* **21**, 230 (1980).
- [13] H. Eslamizadeh, *Int. J. Mod. Phys. E* **24**, 1550052 (2015).
- [14] I. I. Gontchar, A. E. Gettinger, L. V. Guryan, and W. Wagner, *Phys. At. Nucl.* **63**, 1688 (2000).
- [15] I. I. Gontchar, N. A. Ponomarenko, V. V. Turkin, and L. A. Litnevsky, *Phys. At. Nucl.* **67**, 2080 (2004).
- [16] W. Ye, N. Wang, and J. Tian, *Phys. Rev. C* **90**, 041604 (2014).
- [17] H. Eslamizadeh, *Eur. Phys. J. A* **47**, 1 (2011).
- [18] H. Eslamizadeh, *J. Phys. G: Nucl. Part. Phys.* **40**, 095102 (2013).
- [19] J. P. Lestone, *Phys. Rev. C* **59**, 1540 (1999).
- [20] J. P. Lestone and S. G. McCalla, *Phys. Rev. C* **79**, 044611 (2009).
- [21] P. N. Nadtochy, G. D. Adeev, and A. V. Karpov, *Phys. Rev. C* **65**, 064615 (2002).
- [22] A. V. Karpov, P. N. Nadtochy, D. V. Vanin, and G. D. Adeev, *Phys. Rev. C* **63**, 054610 (2001).
- [23] A. V. Karpov, R. M. Hiryanov, A. V. Sagdeev, and G. D. Adeev, *J. Phys. G: Nucl. Part. Phys.* **34**, 255 (2007).
- [24] M. Brack, J. Damgaard, A. S. Jensen, H. C. Puli, and V. M. Strutinsky, *Rev. Mod. Phys.* **44**, 320 (1972).
- [25] A. V. Ignatyuk, M. G. Itkis, V. N. Okolovich, G. N. Smirenkin, and A. S. Tishin, *Yad. Fiz.* **21**, 1185 (1975).
- [26] P. N. Nadtochy and G. D. Adeev, *Phys. Rev. C* **72**, 054608 (2005).
- [27] P. Fröbrich and I. I. Gontchar, *Phys. Rep.* **292**, 131 (1998).
- [28] H. J. Krappe, J. R. Nix, and A. J. Sierk, *Phys. Rev. C* **20**, 992 (1979).
- [29] A. J. Sierk, *Phys. Rev. C* **33**, 2039 (1986).
- [30] R. A. Gherghescu, *Phys. Rev. C* **67**, 014309 (2003).
- [31] R. A. Gherghescu, W. Greiner, and G. Münzenberg, *Phys. Rev. C* **68**, 054314 (2003).
- [32] G. Chaudhuri and S. Pal, *Phys. Rev. C* **63**, 064603 (2001).
- [33] S. Pal and T. Mukhopadhyay, *Phys. Rev. C* **57**, 210 (1998).
- [34] J. Blocki, F. Brut, T. Srokowski, and W. J. Swiatecki, *Nucl. Phys. A* **545**, 511 (1992).
- [35] K. T. R. Davies, A. J. Sierk, and J. R. Nix, *Phys. Rev. C* **13**, 2385 (1976).
- [36] A. A. Seregin, *Yad. Fiz.* **55**, 2639 (1992) [*Sov. J. Nucl. Phys.* **55**, 1473 (1992)].
- [37] K. T. R. Davies, R. A. Managan, J. R. Nix, and A. J. Sierk, *Phys. Rev. C* **16**, 1890 (1977).
- [38] J. Bao, Y. Zhuo, and X. Wu, *Z. Phys. A: Hadrons Nucl.* **352**, 321 (1995).
- [39] R. Vandenbosch and J. R. Huizenga, *Nuclear Fission* (Academic, New York, 1973) p. 427.
- [40] A. Bohr and B. R. Mottelson, *Nuclear Structure* (World Scientific, Singapore, 1998), Vol. 2, p. 748.
- [41] I. Halpern and V. M. Strutinsky, *Proceedings of the United Nations International Conference on the Peaceful Uses of Atomic Energy, Geneva, 1958* (United Nations, Geneva, 1958), Vol. 15, p. 408.
- [42] H. H. Rossner, J. R. Huizenga, and W. U. Schröder, *Phys. Rev. Lett.* **53**, 38 (1984).
- [43] P. D. Bond, *Phys. Rev. C* **32**, 471 (1985).
- [44] H. H. Rossner, J. R. Huizenga, and W. U. Schröder, *Phys. Rev. C* **33**, 560 (1986).
- [45] S. G. McCalla and J. P. Lestone, *Phys. Rev. Lett.* **101**, 032702 (2008).
- [46] T. Døssing and J. Randrup, *Nucl. Phys. A* **433**, 215 (1985).
- [47] J. Randrup, *Nucl. Phys. A* **383**, 468 (1982).
- [48] K. T. R. Davies and J. R. Nix, *Phys. Rev. C* **14**, 1977 (1976).

- [49] M. Oghihara, H. Fujiwara, S. C. Jeong, W. Galster, S. M. Lee, Y. Nagashima, T. Mikumo, H. Ikezoe, K. Ideno, Y. Sugiyama, and Y. Tomita, *Z. Phys. A: Hadrons Nucl.* **335**, 203 (1990).
- [50] B. R. Behera, S. Roy, P. Basu, M. K. Sharan, S. Jena, M. Satpathy, M. L. C. Jee, and S. K. Datta, *Pramana* **57**, 199 (2001).
- [51] V. E. Viola, J. T. D. Thomas, and G. T. Seaborg, *Phys. Rev.* **129**, 2710 (1963).
- [52] S. A. Karamyan, I. V. Kuznetsov, Y. A. Muzycka, Y. T. Oganessian, Y. E. Penionzkevich, and B. I. Pustyl'nik, *Yad. Fiz.* **6**, 494 (1967).
- [53] B. B. Back, R. R. Betts, J. E. Gindler, B. D. Wilkins, S. Saini, M. B. Tsang, C. K. Gelbke, W. G. Lynch, M. A. McMahan, and P. A. Baisden, *Phys. Rev. C* **32**, 195 (1985).
- [54] E. Vulgaris, L. Grodzins, S. G. Steadman, and R. Ledoux, *Phys. Rev. C* **33**, 2017 (1986).
- [55] H. Singh, A. Kumar, B. R. Behera, I. M. Govil, K. S. Golda, P. Kumar, A. Jhingan, R. P. Singh, P. Sugathan, M. B. Chatterjee, S. K. Datta, Ranjeet, S. Pal, and G. Viesti, *Phys. Rev. C* **76**, 044610 (2007).
- [56] A. Saxena, A. Chatterjee, R. K. Choudhury, S. S. Kapoor, and D. M. Nadkarni, *Phys. Rev. C* **49**, 932 (1994).
- [57] M. C. Duijvestijn, A. J. Koning, J. P. M. Beijers, A. Ferrari, M. Gastal, J. van Klinken, and R. W. Ostendorf, *Phys. Rev. C* **59**, 776 (1999).
- [58] V. S. Barashenkov and V. D. Toneev, *Interaction of High Energy Particles and Nuclei with Nuclei* (Atomizdat, Moscow, 1972), p. 566.
- [59] O. E. Shigaev *et al.*, Radium Institut Leningrad Report No. RI-17, 1973 (unpublished).